# Tree crown detection in high resolution optical images during the early growth stages of *Eucalyptus* plantations in Brazil

Jia Zhou
Université Montpellier II
UMR AMAP
Montpellier, France
jia.zhou@cirad.fr

Xavier Descombes, Josiane Zerubia
INRIA
Ariana, INRIA/I3S
Sophia-Antipolis, France

Christophe Proisy, Pierre Couteron
IRD
UMR AMAP
Montpellier, France

Guerric le Maire
Cirad
UMR Eco&Sols
Montpellier, France

Yann Nouvellon
Cirad & USP
UMR Eco&Sols, Atmospheric Sciences Department
São Paulo, Brazil

*Abstract*—**Individual tree detection methods are more and more present, and improve, in forestry and silviculture domains with the increasing availability of satellite metric imagery[2-7]. Automatic detection on these very high spatial resolution images aims to determine the tree positions and crown sizes. In this paper, we use a mathematical model based on marked point processes, which showed advantages w.r.t. several individual tree detection algorithms for plantations [2], to analyze an *Eucalyptus* plantation in Brazil, with 2 optical images acquired by the WorldView-2 satellite. A tentative detection simultaneously with 2 images of different dates (multi-date) has been tested for the first time, which estimates individual tree crown variation during these dates. While, for most current detection methods, only the static state of tree crowns at the moment of one image's acquisition is estimated. The relevance of detection is discussed considering the detection performance in tree localizations and crown sizes. Then, tree crown growth are deduced from detection results and compared with the expected dynamics of corresponding populations.**

***Keywords-tree detection; Eucalyptus plantation; marked point process; multi-date detection***

## I. INTRODUCTION

Tropical plantation forests provide an important share of the global wood supply, where *Eucalyptus* is the most widely planted hardwood genus. In Brazil, eucalyptus plantations occupied a large surface of about 4.3 million ha in 2008. These fast-growing trees have a rotation length of typically 5 to 7 years [8]. Their growth undergoes two periods: expansion of crowns and heights in the first year and development of tree heights in the following years. Monitoring work of this study is mainly realized in the first year.

Monitoring these plantations on large surfaces is rather difficult and requires a lot of trained manpower. The canopy high-resolution images provided by modern satellite-borne remote sensing techniques give another representation of extensive plantations in which individual trees may be documented via the monitoring of the tree crowns. The full uses of these images would help to efficiently analyze and supervise the planting work. The monitoring of the plantation during the first year raises specific questions concerning the detection of trees that die or for which growth is insufficiently fast, because the corresponding locations are to be replanted. It is also important to map areas of bad growth for elucidating the causes of failure. Documenting how the size of the plantation that grows either faster or slower than the average is an indirect mean to define the fertility of the land and the relative performance of the clones and strains that are used.

To do so, we employ the marked point process [1,3] methods to identify every eucalyptus crown.

## II. FIELD INVENTORY

The *Eucalyptus* in this study were planted in November 2009, with a density of about 1670 trees/ha, in São Paulo State, south-eastern Brazil. Over a large area (>200 ha), they were planted in rows, with a distance of about 3 meters between two lines and a distance of about 2m (± 0.5m) between two trees in a line. We selected 4 plantation plots, where field measurements were made concomitantly with the acquisitions

of satellite images: in May and August 2010. In each plot, 84 trees were chosen (14 consecutive trees in a line over 6 consecutive lines) for measurement of the crown diameters in line and inter-line directions, and the distance between two adjacent trees in a line. These data provided ground-truth to assess the crown detection performance. The crown centers of these trees were visually localized in the images by an expert taking into account the external information of approximate tree density and spacing.

## III. VERY HIGH SPATIAL RESOLUTION IMAGES

The two images provided by the WorldView-2 (WV2) satellite are panchromatic and of the spatial resolution: 0.5m. One was acquired on 11th May 2010, centered at (23.031° S, 48.694° W), with the off-nadir angle: 19°, and the target azimuth: 233°. The second was acquired on 1st August 2010, centered at (22.997° S, 48.685° W), with the off-nadir angle: 7°, and the target azimuth: 114°.

Extracts of those images covering the same zone of the monitored plantation at the two successive dates are shown in Fig. 1:

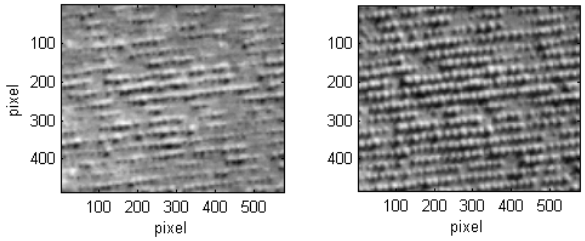


Figure 1. Image extracts of the same zone at two dates (May, August)

## IV. METHOD

### A. Marked point process

We consider a multi-date marked point process to model the plantation both in May and in August [3]. An object in the configuration is defined by a pair of disks (c, $r^{(1)}$, $r^{(2)}$), where $c \in P$ is the center, $r^{(1)}$ is the radius of the tree crown in May and $r^{(2)}$ in August. We assume that $r^{(2)} \geq r^{(1)}$. The object space is given by:

$$\chi = P \times M = [0, X_M] \times [0, Y_M] \times M$$

where $X_M$ and $Y_M$ are the width and length of the images $I_1$ and $I_2$ and:

$$M = \{(r^{(1)}, r^{(2)}) \in [r_m, r_M]: r^{(2)} \geq r^{(1)}\}$$

$r_m$ (respectively $r_M$) is the minimum (respectively maximum) radius of the tree crown.

The marked point process can be expressed by an energy decomposed as the sum of a prior and a data term:

$$U(W) = U_p(W) + U_d(W)$$

where

$$W = \left\{w_i = \left(x_i, y_i, r_i^{(1)}, r_i^{(2)}\right) \in \chi\right\}$$

is a configuration.

We consider a prior penalizing overlaps between neighboring objects:

$$U_p(W) = \gamma_\eta(W)$$

where $\gamma_\eta(W)$ is the number of points of intersecting disks in the image $I_2$ (note that the disks are bigger in the second image).

To define the data energy term, we consider an object based model as follows:

$$U_d(W) = \sum_i W_d(w_i)$$

For each image I, we compute a statistical test $Test_j(c_i, r_i^{(j)})$. To compute the function $Test_j(c_i, r_i^{(j)})$, we consider the set of pixels inside the disk and compute their mean $\mu_i$ and variance $\sigma_i^2$. We also compute the mean $\mu_o$ and variance $\sigma_o^2$ of pixels inside the concentric crown of one pixel width.

If $\mu_i < \mu_o$, then $Test_j(c_i, r_i^{(j)}) = 1$, which means that the disk does not fit a tree, assuming that the tree radiometry is higher on the ground. Otherwise, we compute a Student test:

$$S_j\left(c_i, r_i^{(j)}\right) = \frac{\mu_i - \mu_o}{\sqrt{\frac{n_i\sigma_i^2 + n_o\sigma_o^2}{n_i + n_o - 2}}\sqrt{\frac{1}{n_i} + \frac{1}{n_o}}}$$

We then compute the p-value $p_j(c_i, r_i^{(j)})$ associated with this statistical test and consider a threshold t, as a parameter. Then the data term is written as follows:

$$Test_j\left(c_i, r_i^{(j)}\right) = \begin{cases} \dfrac{t - p_j(c_i, r_i^{(j)})}{t}, & if\ p_j\left(c_i, r_i^{(j)}\right) > 1 - t \\ p_j\left(c_i, r_i^{(j)}\right) - 1, & otherwise \end{cases}$$

Therefore, an object fits the data if the p-value is smaller than 1-t.

To use the information of both images, we assume that a tree should be detected if the test function is negative in at least one image. Therefore, we define the data term as follows:

$$u_d(w_i) = \left[\max\left(-Test_1\left(c_i, r_i^{(1)}\right), 0\right) + max\left(-Test_2\left(c_i, r_i^{(2)}\right), 0\right)\right] \times sign\left(\min\left(Test_1\left(c_i, r_i^{(1)}\right), Test_2\left(c_i, r_i^{(2)}\right)\right)\right)$$

To optimize the model, we consider a simulated annealing based on a multiple birth and death process (MBD). This process has first been proposed in [1].

The algorithm simulating the process is defined as follows:

1. Initialize the temperature parameter T = 1, the birth rate $\delta = \frac{X_M \times Y_M}{r_M}$ and alternate birth and death steps.
2. Birth step: for each pixel s in the image I, if there is no disk centered in s, we add an object in s, with a random radius between $r_m$ and $r_M$, with probability B(s), where B(s) is proportional to δ and the data term in s (see [9] for details).

3. Sorting step: once the birth step is finished, we compute the data term Test($w_i$) for each object in the current configuration of objects. Then, we sort them, in decreasing order, according to their data energy.
4. Death step: for each object xi taken in this order, we compute the death rate as follows:

$$d(w_i) = \frac{\delta \times a(w_i|w)}{1 + \delta \times a(w_i|w)} \quad , \quad \text{where :}$$

$$a(w_i|w) = exp\left[\frac{\gamma \times \eta(w_i|w) + test(w_i)}{T}\right]$$

and $\eta(w_i|w)$ being the number of disks in W intersecting $w_i$.

5. Convergence: if the process has not converged, which means than the configuration has changed during the last iterations, then decrease T and δ, according to a law defined in [1], and go back to step 2.

### B. *Detection score*

To assess the detection results in tree numbers and positions compared to the field reference, we used a score which was already introduced in [2] for comparing different tree crown detection algorithms. For this, a matching work has to be made first between the detected disk set and the reference tree set, then the successful detection number, the omission and false detection number can be calculated. For a reference tree be considered to be detected by a disk (a successful detection), the disk center should fall within the extent of the corresponding tree crown. A reference tree can be matched with only one disk, and other disks not matched are considered as false detections. A tree not matched with any disk is considered as an omission. The detection score is defined as follows:

$$score = 100 * \frac{N_s}{N_s + N_o + N_c}$$

where Ns is the successful detection number, No is the omission number and Nc the false detection number.

### C. *Interpolation*

The sizes of planted *Eucalyptus* crowns are first limited by the space between adjacent trees in the same line because of competition for spaces. The limitation between two lines occurs later. The diameters in the inter-line direction begin to exceed that in line direction in the first year of plantation. Nevertheless, the mean diameters (the arithmetic means of diameters in two directions) exceed rarely 2.7m. Furthermore, the field measurements of diameters were based on the branches which extend the most from the crowns center in the line and inter-line directions, and may often be not visible in the images. Thus, in the 0.5m resolution images, a tree crown covers just a few pixels, with a radius length of 1 or 2 pixels. These small crowns make it difficult for the marked point processes to give correct detections both in position and in crown size. We were working in the limited conditions for these young populations. Better resolution images are needed for more detailed analysis.

A solution to this problem is the resampling of the original images by interpolation. The usual interpolation methods [10] for images like nearest-neighbors, bilinear, and bicubic were tested at different scales between 2 and 10. The detection works better on the interpolated images, usually when they were resampled at 5, which means at the resolution of 0.1m. The detection results were little influenced by the choice of interpolation method. Therefore, we will just show the results on the bilinear interpolated images in the following.

## V. RESULTS

The detection results were first analyzed in terms of tree number, Table 1 contains the list of statistics in each plot. On the whole, the detection is encouraging for tree number counting. For each plot, almost all the reference trees were detected (between 89% and 95%) with just a few false detections (between 0 and 1.3%). The detection in crown position and delineation of one plot are shown in Fig. 2.

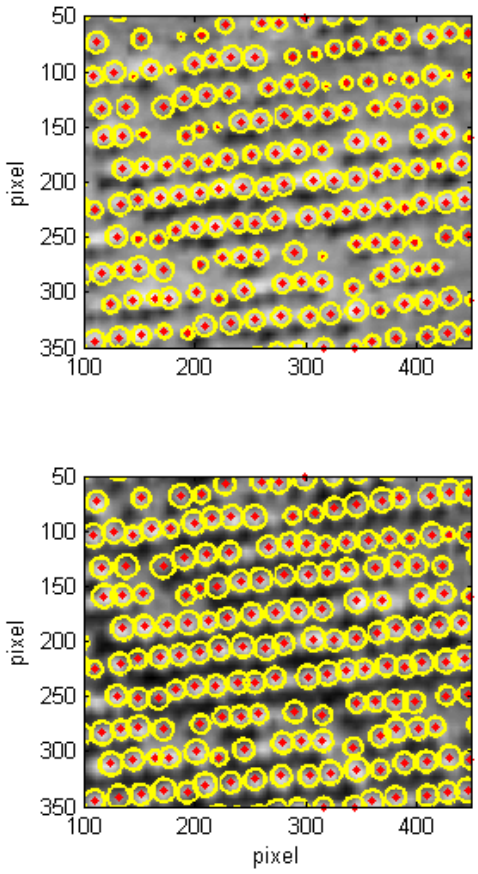


Figure 2. Detection result in May (on the top) and in August (at the bottom) of one plot. The points represent detected tree positions, and the circles represent delineated crowns.

For the crown size estimation, we compared, for every detected tree in the reference zones, the estimated average

crown diameter given by the process with the measured crown diameter in the field. In Fig. 3, we can see these comparisons of diameters in 4 plots. Note that the precision of estimated crown diameters depends on the image resolution, so the minimum difference between successive diameter values is twice the spatial resolution of the image interpolated with bilinear method. However, without taking this into account, many points in the scatter graphs were still away from the line x=y. The dashed lines built an interval of [-0.5m, 0.5m] around the line x=y, with 0.5m corresponding the image resolution.

When considering the scatter graph of August, the clouds of points were moved a little to the right, which means that in these plots, the detection process tended to underestimate the crown sizes. This phenomenon is related, on one hand, to the fact that the measurement of diameters in the field was based on the branches which extended the most from the crown centers, but were not always detectable on images, as we mentioned earlier; and on the other hand, to a weakness of the detection model, in which a tree crown is simply modeled by a disk. Indeed, real tree crowns are not perfect disks, thus crowns touched each other along the line direction and extended more in the inter-line direction, which was the case in August. The penalization of large overlapping of disks in the detection algorithm, with purpose of avoiding false detections, disfavors big disks in this case. The diameters of big disks are usually limited by the distances between adjacent trees in a line (if the crowns are touching each other in the line direction), which were about 1.9m according to field measurements, while the mean of measured diameters were about 2.1m in August.

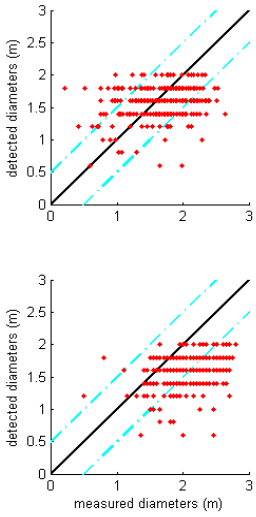


Figure 3. Comparisons of the average diameters of the detected tree crowns with field measured crown diameters in May (on the top) and in August (at the bottom) of 4 plots.

From the detected crown diameters in May and in August, the crown growths were deducted for individual trees, which are represented in Fig. 4 as histograms. Compared with the field measurements in Fig. 5 (with the modes at 0.4~0.5m), we note that these growths were widely underestimated (with the modes at 0.2~0.3m in Fig.4). However, it was impossible to get a better accuracy on crown diameter estimation with these two images which are limited in spatial resolution, so the estimations of crown growths were also influenced.

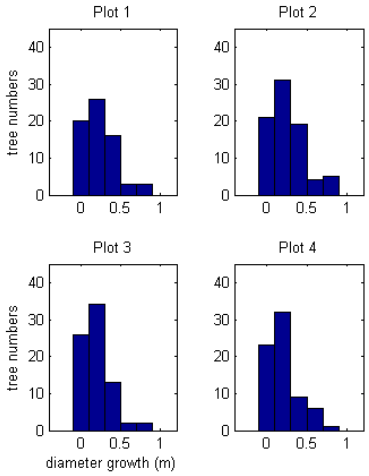


Figure 4. Distributions of detected growths in 4 plots.

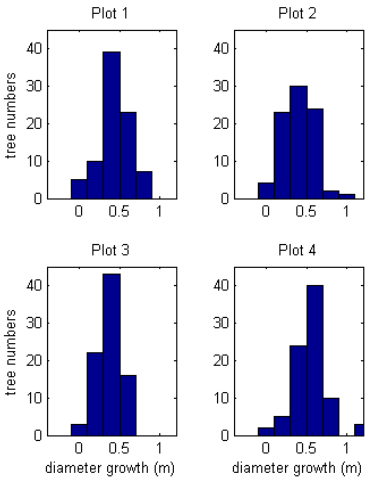


Figure 5. Distributions of measured growths in 4 plots.

TABLE 1. Statistics of detection results in 4 plots

| Plot | Tree number | Detected tree number | Successful detections | % detected trees | False detections | % false detections | Detection scores |
|---|---|---|---|---|---|---|---|
| 1 | 83 | 75 | 74 | 89.2 | 1 | 1.3 | 88.1 |
| 2 | 84 | 79 | 79 | 94.0 | 0 | 0 | 94.0 |
| 3 | 84 | 77 | 77 | 91.7 | 0 | 0 | 91.7 |
| 4 | 83 | 80 | 79 | 95.2 | 1 | 1.3 | 94.0 |

## VI. DISCUSSION

In this study, we were in the limited case of the young *Eucalyptus* stage analysis (owing to the ratio of crown sizes and the image resolution), using satellite images of spatial resolution 0.5m. Although interpolation methods could improve detection results, they were not the solution to the essential problem of resolution limit, because noise might be introduced during the interpolation process. The detected crown sizes were of the same order of magnitude as the measured sizes in the field, however, an accuracy of better than 0.5m cannot be asked. During the period between the two images in this study (81 days), the best crown growth was about 0.7m in diameter, which was not detectable with these images. But, the detection results remain consistent with the dynamics of the young eucalyptus population, which shows the potential of our detection method.

We also tried to apply the method on other population of tropical forest stands, as natural mangrove forest in French Guiana, where detections were much more difficult owing to the complexity and high vegetation density of the population. In addition, to better test and adjust the new method, we used the simulated optical DART (Discrete Anisotropic Radiative Transfer) images [11,12], where exact field inventory could be provided for detection analysis.

## ACKNOWLEDGMENT

These satellite images were acquired within the ORFEO program, a CNES Accompaniment Program for the use of PLEIADES images. We acknowledge this project for funding the images, and Claire Tinel (CNES) for her help with the images acquisitions. We are grateful to the Eucflux project (http://www.ipef.br/eucflux/) for providing the inventories of the eucalyptus plantation plots.

## REFERENCES

[1] X. Descombes, R. Minlos, and E. Zhizhina, “Object extraction using a stochastic birth-and-death dynamics in continuum," J Math Imaging Vis 33, 347-359 (2009).

[2] M. Larsen, M. Eriksson, X. Descombes, G. Perrin, T. Brandtberg and F. A. Gougeon, “Comparison of six individual tree crown detection algorithms evaluated under varying forest conditions”, International Journal of Remote Sensing (to appear).

[3] J. Zhou, C. Proisy, X. Descombes, I. Hedhli, N. Barbier, J. Zerubia, J. P. Gastellu-Etchegorry and P. Couteron, ”Tree crown detection in high resolution optical and LiDAR images of tropical forest”, Proc. of SPIE Vol. 7824, 78240Q (2010).

[4] C. J. Prost, M. D. Dare and A. Z. Zerger, “Discrimination of Eucalyptus canopy from airborne linescanner imagery using Markov random field modeling”, Environmental Modelling & Software 23(2008) 56-71.

[5] G. Perrin, “Etude du couvert forestier par processus ponctuels marqués”, PhD thesis, Université de Nice Sophia-Antipolis, France, 2006.

[6] J. Holmgren, A. Persson and U. Söderman, “Species identification of individual trees by combining high resolution lidar data with multispectral images”, International Journal of Remote Sensing, 29: 1537-1552,2008.

[7] M. Erikson, “Segmentation and Classification of Individual Tree Crowns in High Spatial Resolution Aerial Images”, PhD thesis, Swedish University of Agricultural Sciences, 2004.

[8] G. Le Maire, C. Marsden, W. Verhoef, F. J. Ponzoni, D. Lo Seen, A. Bégué, J. L. Stape and Y. Nouvellon, “Leaf area indix estimation with MODIS reflectance time series and model inversion during full rotations of Eucalyptus plantations”, Remote Sensing of Environment, 115 (2011) 586-599.

[9] S. Descamps, X. Descombes, A. Béchet and J. Zerubia, “Flamingo detection using marked point processes for estimating the size of populations”, Traitement du Signal 26, (2009) 95-108 .

[10] P. Thévenaz, T. Blu and M. Unser, “Image Interpolation and Resampling”, Handbook of Medical Image Processing and Analysis (Second Edition), Pages 465-493, 2009.

[11] J. Gastellu-Etchegorry, P. Guillevicl, F. Zagolski, V. Demarez, V. Trichon, D. Deering and M. Leroy, “Modeling brf and radiation regime of tropical and boreal forests: Brf”, Remote Sensing of Environment, 68, (1999) 281-316.

[12] V. Bruniquel-Pinel and J. Gastellu-Etchegorry, “of texture of high resolution images of forest to biophysical and acquisition parameters”, Remote Sensing of Environment, 65(1), (1998) 61-85.